Scaling property of the heat-current flows across a weak interface

Lei Wang (王雷)* and Yanjiang Guo (郭彦江)
Department of Physics and Beijing Key Laboratory of Opto-electronic Functional Materials and Micro-nano Devices, Renmin University of China, Beijing 100872, People's Republic of China

(Received 3 August 2018; published 3 October 2018)

We systematically study heat current J that flows through a few one-dimensional nonlinear lattices, each of which consists of two identical segments that are coupled by a weak interface. Existing theoretical analyses expect that J is generally proportional to the square of the interface strength when the temperature drop is fixed and small. However, we observe two completely different classes in our numerical simulations. One follows the original expectation. In the other class, however, J follows a power-law decay with the strength and the detailed power exponent depends on the details of the lattices and the interface interaction. Further theoretical analyses reveal that in the former class the interface potential energy decays with the interface strength linearly, which is commonly observed. In the latter class, the interface potential energy approaches a constant that is independent of the interaction strength. The detailed power exponents are then well explained.

DOI: 10.1103/PhysRevE.98.042108

I. INTRODUCTION

When heat flows through an interface between two materials, an interface thermal resistance (ITR) must be overcome [1]. ITR was once regarded as negligible, until 1941 Kapitza reported the temperature jump near the boundary between helium and a solid when heat flows across it [2,3]. Such a thermal boundary resistance is then often called as a Kapitza resistance. Later, the acoustic mismatch model [4] and diffuse mismatch model [5], which assume no phonon scattering at interface, and all phonons incident on the interface will scatter, were proposed to describe the solid-liquid and solid-solid interfaces, respectively. The related topics have attracted much interest in the past decades.

In the application aspect, recent successes in fabrication of nanoscale materials have enabled us to control heat flow intelligently in microscopic scale. With the successfully proposed toy models of thermal diode [6–8] that rectifies heat flow, thermal transistor that switches and modulates heat flow [9], thermal logic gates that realize all fundamental logic operations [10], and thermal memory that stores information by heat [11], etc., information carrying and processing by heat has become theoretically possible [12]. Some nanoscale thermal devices have also been experimentally realized, e.g., a phonon waveguide [13] and a thermal rectifier by nanotubes [14]. It is worth mentioning that the physical underlying mechanism of many of the above-mentioned thermal devices is that the ITR depends on the match-mismatch of the phonon spectra at the interface sensitively [8], in particular when the interface is very weak.

Besides the phonon spectra, the strength of the interface is another important factor that controls the heat flow largely. It is easily understood that generally the weaker the interface interaction the smaller the heat current. The detailed dependence is not so straightforward and has been rarely studied. It has been observed by numerical simulation that J flows through a weak interface in a model of thermal diode that consists of two Frenkel-Kontorova (FK) [7] segments, decays with the interface strength $k_{\rm int}$ by $k_{\rm int}^2$ in the small $k_{\rm int}$ limit. Recently, such a $k_{\rm int}^2$ law has been proven analytically and claimed as a general relation that is independent of any detail of segment materials and interface [15].

In this paper we shall investigate systematically the generality of the above-mentioned $k_{\rm int}^2$ law in a serial of one-dimensional (1D) nonlinear lattice models and reveal that although such a law is correct in a wide class of models, there still exists at least another class of models in which the law is violated. In that class, J still satisfies a power-law decay with $k_{\rm int}$ by $k_{\rm int}^\alpha$. The detailed power exponent α does, however, depend on the details of the materials and the interface.

The paper is organized as follows. The lattice models and interfaces that we shall study are introduced in Sec. II. Numerical simulation results for those models and interfaces are presented in detail in Sec. III. Theoretical analyses that explain all the numerical findings are presented in Sec. IV. Conclusions and remarks are in Sec. V.

II. LATTICE MODELS AND INTERFACE INTERACTIONS

Each 1D nonlinear lattice that we shall study consists of two identical bulk segments that are connected through a weak interface interaction. The Hamiltonian of a whole system takes the general form

$$\begin{aligned} H &= H_L + H_{\rm int} + H_R \\ &= \sum_{i=1}^{N/2}\left[\frac{\dot{x}_i^2}{2} + V(x_i - x_{i-1}) + U(x_i)\right] \\ &\quad + V_{\rm int}(x_{N/2+1} - x_{N/2}) \\ &\quad + \sum_{i=N/2+1}^{N}\left[\frac{\dot{x}_i^2}{2} + V(x_{i+1} - x_i) + U(x_i)\right]. \end{aligned} \tag{1}$$

*phywanglei@ruc.edu.cn

The mass of all particles has been set to unity and we have already assumed that the left and right segments take the same form and both of them consist of $N/2$ particles with N an even number. When necessary, two different kinds of boundary conditions (BC) shall be considered, i.e., the fixed BC ($x_0 = x_{N+1} = 0$) and the free BC ($x_0 = x_1$ and $x_{N+1} = x_N$). Three representative types of lattices will be studied. They are: (1) the ϕ^4 lattice [16] with $V(x) = \frac{1}{2}x^2$ and $U(x) = \frac{1}{4}x^4$, (2) the coupled rotator lattice with $V(x) = 2.5[1 - \cos(x)]$ [17] and $U(x) = 0$, and (3) the Fermi-Pasta-Ulam(FPU)-β lattice [18] with $V(x) = \frac{1}{2}x^2 + \frac{1}{4}x^4$ and $U(x) = 0$. The temperatures in these studies are around 1. Heat conduction in a ϕ^4 lattice is normal due to the on-site potential that breaks the total momentum conservation, which is typically a necessary condition for a normal heat conduction in 1D systems. At such a temperature heat conduction in the coupled rotator lattice is normal too. It is one of the very seldom exceptions that a 1D system without an on-site potential has a normal heat conduction. Heat conduction in the FPU-β segment is divergent. It is also a very presentative example showing that without an on-site potential, nonlinearly alone is generally not sufficient to induce a normal heat conduction in 1D systems [19,20].

The interface interactions also include three representative types: (1) the nonlinear quartic interaction that $V_{\rm int}(x) = k_{\rm int}\frac{1}{4}x^4$, (2) the linear interaction that $V_{\rm int}(x) = k_{\rm int}\frac{1}{2}x^2$, and (3) the rotator interaction that $V_{\rm int}(x) = k_{\rm int}[1 - \cos(x)]$. We shall reveal that the detailed type of interaction does play an important role in determining the decay properties of the heat current J even in the small interface strength $k_{\rm int}$ limit.

In the numerical simulations, two Langevin heat baths with slightly different temperatures 1.1 and 0.9 are coupled to the left and right ends of the lattice, i.e., the first and Nth particles. Average heat current J that flows through the lattice is then calculated after the system reaches a stationary state. The damping coefficient γ of the heat baths is always set to 2, unless otherwise stated in Sec. III C 3, where we shall study its role. A fifth-order Runge-Kutta algorithm [21], which provides a high cost-effect, is applied for the calculation.

III. NUMERICAL SIMULATIONS

A. The ϕ^4 lattice

The first lattice that we study consists of two ϕ^4 segments. The results of this lattice are simple. The temperature profiles for the quartic interface and different values of $k_{\rm int}$ are plotted in Fig. 1(a). We see when $k_{\rm int}$ is small enough, temperature profiles in the two segments are flat, which implies that the temperature jump at the interface is basically the value of the whole temperature difference of the two heat baths. In such a situation, heat resistance in the two segments is negligible. We shall not plot the temperature profiles for the other two lattices, since the pictures are similar. In Fig. 1(b) the heat current J versus the strength of interface interaction $k_{\rm int}$ for various types of interface interaction and length of lattice $N = 32$ and 64 are plotted. The data for different N basically overlap each other, which confirms the fact again that the bulk heat resistance can be ignored. In the small $k_{\rm int}$ limit, J follows $k_{\rm int}^2$ exactly, i.e., the $k_{\rm int}^2$ law holds. The BC is fixed and we have checked that it does not affect the results.

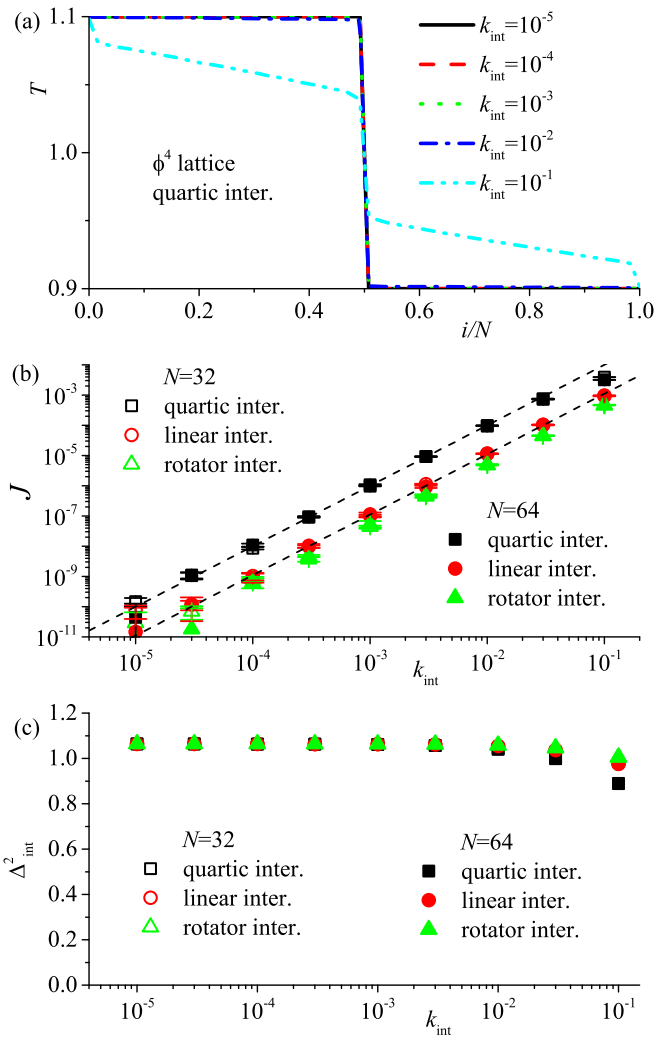

FIG. 1. (a) Temperature profiles in the ϕ^4 lattice with quartic interface. $N = 64$. (b) Heat current J versus $k_{\rm int}$ for various interface and lattice length N. The error bars are basically invisible, except for some data with very small $k_{\rm int}$. Dashed lines with slope 2 are drawn for reference. (c) The mean square relative displacement between the interface particles $\Delta^2_{\rm int}$ versus $k_{\rm int}$ for various interface. Open and solid symbols are for N = 32 and 64 in all the figures.

For further study and comparison, the mean square relative displacement between interface particles $\Delta^2_{\rm int} \equiv \langle (x_{N/2+1} - x_{N/2})^2 \rangle$ is also plotted in Fig. 1(c). The physical meaning of $\Delta^2_{\rm int}$ is clear. It measures the relative movement of the two interface particles, and the larger the magnitude of relative movement the larger the $\Delta^2_{\rm int}$. It can be easily seen and understood that due to the hard [22] on-site potential $U(x)$, the particles can only vibrate around their equilibrium positions. Therefore, $\Delta^2_{\rm int}$ depends on $k_{\rm int}$ only very slightly and approaches a temperature-dependent constant in the no-link ($k_{\rm int} \to 0$) limit.

B. The coupled rotator lattice

The second lattice we shall study is the coupled rotator lattice. In Fig. 2(a) the heat current J versus the strength of interface interaction $k_{\rm int}$ for various types of interface

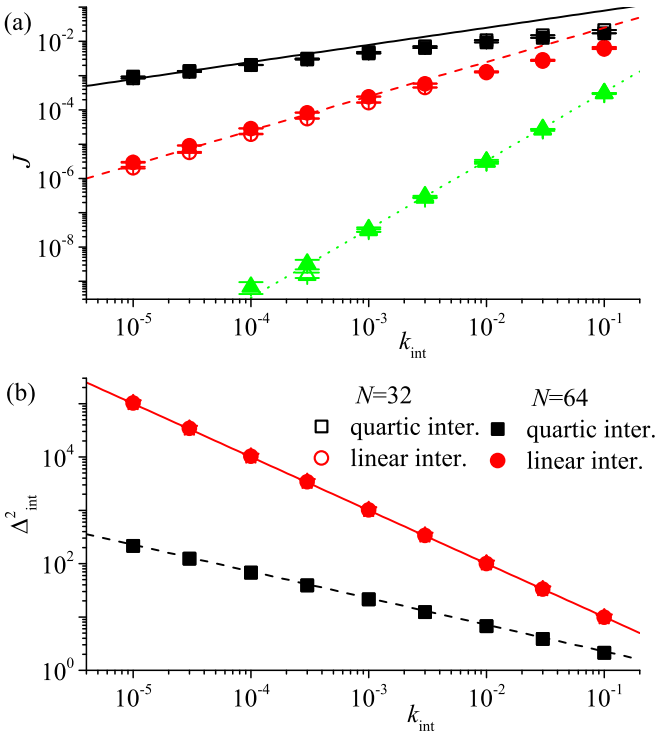

FIG. 2. The coupled rotator lattice with free BC. (a) Heat current J versus $k_{\rm int}$ for various interfaces and lattice length N. The symbol groups from the top down are for the quartic, the linear, and the rotator interfaces, respectively. The error bars are basically smaller than the symbol size. The solid, dashed, and dotted lines with slope 0.5, 1, and 2, respectively, are drawn for reference. (b) The mean square relative displacement between the interface particles $\Delta^2_{\rm int}$ versus $k_{\rm int}$ for the the quartic and the linear interfaces. That for the rotator interface is not plotted since it diverges. Solid and dashed lines are with slope -1 and -0.5. Open and solid symbols are for $N = 32$ and 64 in all the figures.

interaction and length of lattice $N = 32$ and 64 are plotted. In the small $k_{\rm int}$ limit, J always follows a power-law dependence on $k_{\rm int}$, i.e.,

$$J \sim k_{\rm int}^{\alpha}. \tag{2}$$

However, the detailed value of α varies for different interface interactions. For the quartic, the linear, and the rotator interactions, $\alpha = 0.5$, 1, and 2, respectively. Only the last case is originally expected. In the figure only the results for free BC are plotted but we have checked again that it does not affect the conclusions for this lattice.

In contrast to the case in Fig. 1(b), $\Delta^2_{\rm int}$ plotted in Fig. 2(b) follows a power-law dependence on $k_{\rm int}$, i.e.,

$$\Delta^2_{\rm int} \sim k_{\rm int}^{-\beta}, \tag{3}$$

and approaches infinity in small $k_{\rm int}$ limit, where $\beta = 0.5$ and 1 for the quartic and linear interface interactions, respectively. In these hard interface cases, the $k^2_{\rm int}$ law is violated. As for the rotator interface, since interactions in both the segments and the interface are soft, $\Delta^2_{\rm int}$ diverges in the long time limit. In this case, the $k^2_{\rm int}$ law holds.

C. The FPU-β lattice

The third lattice we shall study is the FPU-β lattice. Upon understanding the cases in the previous two lattices, the case in this lattice, although is much more complicated, can be well explained. In the following we study the roles of different factors in this lattice.

1. The role of the interface interaction

We first study the cases for free BC, which is relatively simple. In Fig. 3(a) the heat current J versus $k_{\rm int}$ for various types of interface interaction and length of lattice $N = 32$ and 64 are plotted. Again the length N plays only invisible role. In the small $k_{\rm int}$ limit, J follows again a power-law dependence on $k_{\rm int}$ and $\alpha = 0.5$, 1, and 2, respectively, for the quartic, the linear, and the rotator interfaces. Only the last one meets the original expectation.

As for the mean square relative displacement between the interface particles $\Delta^2_{\rm int}$ that is plotted in Fig. 3(b), it follows a power-law with $\beta = 0.5$ and 1 for the quartic and linear interface interactions, respectively. All these above results are similar to those for the coupled rotator lattice.

2. The role of the boundary conditions and lattice length N

Figures 3(c) and 3(d) are for the fixed BC. In Fig. 3(c) we see that in the not-very-small $k_{\rm int}$ regime, J basically follows the same power-law dependence as it does in the free BC cases. However, in the small $k_{\rm int}$ limit, all the power exponents approach 2. The picture for the $\Delta^2_{\rm int}$ that is plotted in Fig. 3(d) is also quite similar. It follows the similar slopes as it does in the free BC case in large $k_{\rm int}$ regime. In the small $k_{\rm int}$ limit, however, $\Delta^2_{\rm int}$ approaches constants, and the longer the lattice, the larger the constants.

3. The role of the heat bath damping coefficient γ

Heat current J in the FPU-β lattice versus $k_{\rm int}$ for the heat bath damping coefficient $\gamma = 0.5$ and 2.0 are depicted in Fig. 4(a). It is observed with surprise that it depends so greatly on γ, even in the small $k_{\rm int}$ limit. In very large $k_{\rm int}$ regime, the larger γ induces a larger J. While in the very small $k_{\rm int}$ cases, it reverses. The smaller value of $\gamma = 0.5$ induces a much larger J, which is about four times of that with $\gamma = 2.0$. However, the power-law dependence on $k_{\rm int}$ remains unchanged. The power exponent α keeps 0.5 and 1 for the quartic and linear interface interactions, respectively. In order to confirm it we have to extend the calculation to extremely small values of $k_{\rm int}$.

To understand the above finding, we have calculated the power spectra of the two interface particles in the no-link ($k_{\rm int} = 0$) cases. The results plotted in Fig. 4(b) and 4(c) reveal that in the case $\gamma = 0.5$ the power spectra concentrate much more on the low frequency regime. It is well known that low frequency phonons carry heat energy much more efficiently than the high frequency ones do. This well explains the resulted much larger heat current in the quartic and the linear interface cases. The case for the rotator interface is quite different. This mechanism lose its effectiveness completely because low frequency phonons cannot carry energy across

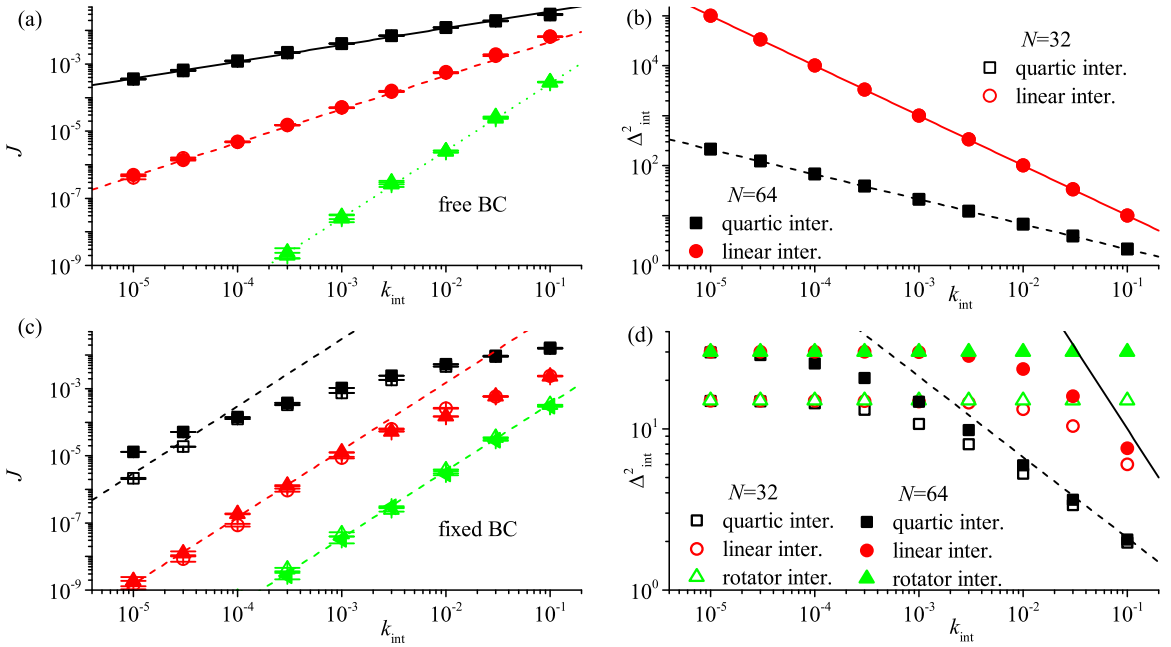

FIG. 3. Upper row: FPU lattices with free BC. (a) Heat current J versus $k_{\rm int}$ for various interfaces and lattice length N. The symbol groups from the top down are for the quartic, the linear, and the rotator interfaces, respectively. Solid, dashed, and dotted lines with slope 0.5, 1, and 2, respectively, are drawn for reference. (b) $\Delta^2_{\rm int}$ versus $k_{\rm int}$ for the quartic (squares) and the linear (circles) interfaces. That for the rotator interface is not plotted since it diverges. Solid and dashed lines are with slopes -1 and -0.5. Lower row: FPU lattices with fixed BC. (c) Heat current J versus $k_{\rm int}$ for various interfaces and lattice length N. The symbol groups from the top down are for the quartic, the linear, and the rotator interfaces, respectively. Open and solid symbols are for $N = 32$ and 64. Lines with slope 2 are drawn for reference. (d) $\Delta^2_{\rm int}$ versus $k_{\rm int}$ for the quartic (squares), the linear (circles), and the rotator (triangles) interfaces. Solid and dashed lines are with slopes -1 and -0.5. Open and solid symbols are for $N = 32$ and 64 in all the figures.

such a soft interface at all. As a consequence, heat current J for different γ is basically the same.

IV. THEORETICAL ANALYSES

It is quite clear that the behaviors of $\Delta^2_{\rm int}$ directly connect to how the heat current J decays with $k_{\rm int}$. The relation between the two power exponents α and β is plotted in Fig. 5(a). Apparently there exist two completely different classes, class one is $\alpha = 2$ and $\beta = 0$, and class two follows $\alpha = \beta$.

The class one includes (1) the ϕ^4 lattice, (2) the FPU lattice with fixed BC, and (3) all the lattices with rotator interface. The case (1) is a lattice with hard on-site potential. In such a case, all the particles including the two interface particles are confined, i.e., each of them can only vibrate around a center with a temperature-dependent finite magnitude. Therefore, the probability distribution functions (PDF) of the relative displacement between the two interface particles approaches a $k_{\rm int}$-independent asymptotic distribution $P(\Delta x)$ in the small $k_{\rm int}$ limit, where $\Delta x \equiv x_{N/2+1} - x_{N/2}$. Since the interface potential energy takes the general form $V_{\rm int}(\Delta x) = k_{\rm int} f(\Delta x)$, its average value $\langle H_{\rm int}\rangle$ in the limit follows

$$\langle H_{\rm int}\rangle = \int_{-\infty}^{-\infty} V_{\rm int}(\Delta x)P(\Delta x)d\Delta x = k_{\rm int}\int_{-\infty}^{-\infty} f(\Delta x)P(\Delta x)d\Delta x. \quad (4)$$

Apparently, the last integral is finite, non-zero, and $k_{\rm int}$-independent. $\langle H_{\rm int}\rangle$ thus decays with $k_{\rm int}$ linearly. $\Delta^2_{\rm int}$ approaching a constant can also be explained similarly.

The case (2) is a hard inter-particle potential plus fixed BCs. Although there is no on-site potential, the fixed BCs can also confine all the particles through their hard inter-particle interactions. This time, in a finite lattice each interface particle can vibrate around a center with a temperature-dependent and also lattice-length-dependent finite magnitude. The above analyses also apply thus $\langle H_{\rm int}\rangle$ still decays with $k_{\rm int}$ linearly.

Case (3) is quite different. In this case, $f(\Delta x)$ is periodic and finite. The period equals 2π for the rotator interface that we studied. Then in the small $k_{\rm int}$ limit, although $P(\Delta x)$ possibly does not exist if any of the two interface particles is not confined, $P(\{\Delta x\})$ must exist and approach a $k_{\rm int}$-independent asymptotic distribution, where $\{x\} \equiv x - [\frac{x}{2\pi}]2\pi$, and $[x]$ denotes the largest integer that is no greater than x. Therefore,

$$\langle H_{\rm int}\rangle = \int_0^{2\pi} V_{\rm int}(\{\Delta x\})P(\{\Delta x\})d\{\Delta x\} = k_{\rm int}\int_0^{2\pi} f(\{\Delta x\})P(\{\Delta x\})d\{\Delta x\}. \quad (5)$$

Again, the last integral is finite, non-zero, and $k_{\rm int}$-independent, so that $\langle H_{\rm int}\rangle$ decays with $k_{\rm int}$ linearly. The $k^2_{\rm int}$ law holds in all those three above cases.

The class two includes the FPU lattice with free BC and the coupled rotator lattice. The interface interaction must be hard. In those cases since the interface particles are not confined,

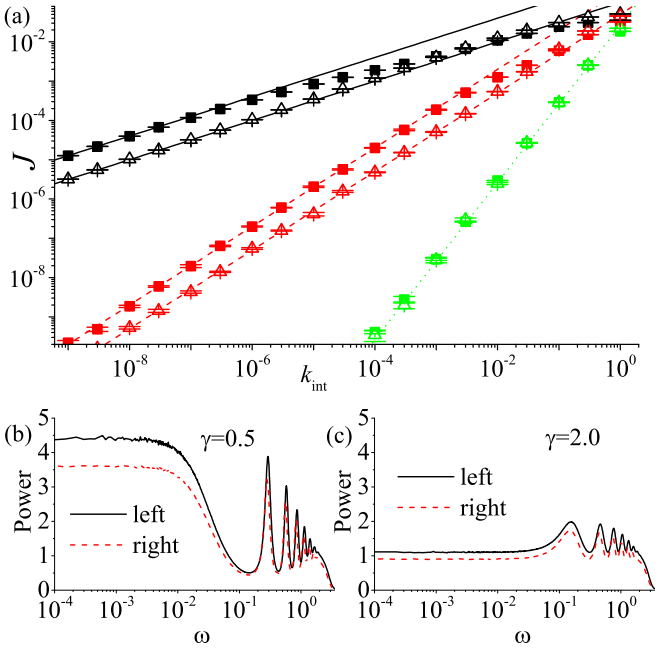

FIG. 4. (a) Heat current J for the FPU-β lattice versus $k_{\rm int}$ with various interfaces and heat bath γ. $N = 32$. The black, red, and green symbol groups from the top down are for the quartic, the linear, and the rotator interfaces, respectively. Solid squares and open triangles are for $\gamma = 0.5$ and 2. The error bars are basically smaller than the symbol size. Solid, dashed, and dotted lines are with slopes 0.5, 1, and 2, respectively. (b) and (c) Power spectra of the two particles left and right to the interface, for $\gamma = 0.5$ and $\gamma = 2$, in the no-link case.

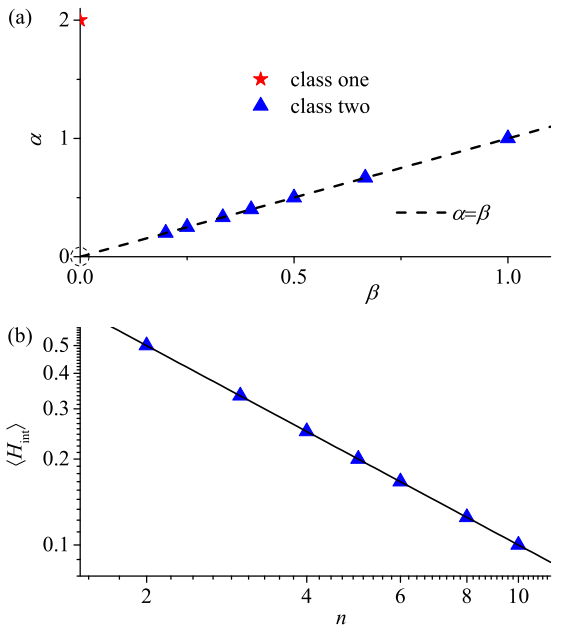

FIG. 5. (a) The dependence of the two power exponents α and β. The dashed line refers to $\alpha = \beta$. Class one includes: (1) the ϕ^4 lattice, (2) the FPU lattice with fixed BC, and (3) all the lattices with rotator interface. Class two includes: hard interfaces that takes the general form $V_{\rm int}(x) = k_{\rm int}\frac{1}{n}|x|^n$, between (1) the rotator lattice and (2) the FPU lattice with free BC. The point $\alpha = \beta = 0$, which is surrounded by the dashed circle, indicates the limiting case for $n \to \infty$. (b) Average interface potential energy $\langle H_{\rm int}\rangle$ versus n for the H_n type interface in class two. The solid line refers to $\langle H_{\rm int}\rangle = \frac{1}{n}$.

$P(\Delta x)$ does not exist in the small $k_{\rm int}$ limit, and because $f(\Delta x)$ is non-periodic the analyses in Eq. (5) do not apply. Therefore, $\langle H_{\rm int}\rangle$ no longer decays with $k_{\rm int}$ linearly. In our studies, all the hard interactions take the general H_n form $V_{\rm int}(x) = k_{\rm int}\frac{1}{n}|x|^n$. In Fig. 5(a), the results for the FPU lattice with free BC and various n are plotted. Besides the linear and quartic interactions that have been discussed in previous sections, interactions with other values of $n = 3$, 5, 6, 8, and 10 are also included. All the results satisfy $\beta = 2/n$ and $\alpha = 2/n$ perfectly. Therefore, $\alpha = \beta$.

$\beta = 2/n$ can be understood by assuming that the average interface potential energy $\langle H_{\rm int}\rangle$ keeps a constant independent of the interface coupling strength $k_{\rm int}$. Such an assumption has also been confirmed by our numerical simulation. The agreement is exact again. Then it is easily proven that $\Delta^2_{\rm int}$ diverges to infinity in the small $k_{\rm int}$ limit by $k_{\rm int}^{-\frac{2}{n}}$.

Furthermore, we have also plotted the values of $\langle H_{\rm int}\rangle$ for various n in Fig. 5(b). All the data, up to $n = 10$, follow $1/n$ exactly. This result agrees with the following analytical expectation for bulk materials with the temperature $T = 1$ [23].

Consider an infinite long lattice with periodic BC and all H_n type inter-particle interaction, i.e., the Hamiltonian reads

$$H = \sum_i \left[\frac{1}{2}m\dot{x}_i^2 + \frac{k}{n}(x_i - x_{i-1})^n\right]. \tag{6}$$

In an equilibrium state,

$$\begin{aligned} T &= \left\langle x_i \frac{\partial H}{\partial x_i}\right\rangle = k\langle x_i[(x_i - x_{i-1})^{n-1} - (x_{i+1} - x_i)^{n-1}]\rangle \\ &= k\langle x_i[(x_i - x_{i-1})^{n-1}] - x_i[(x_{i+1} - x_i)^{n-1}]\rangle \\ &= k\langle x_i[(x_i - x_{i-1})^{n-1}] - x_{i-1}[(x_i - x_{i-1})^{n-1}]\rangle \\ &= k\langle (x_i - x_{i-1})^n\rangle = n\langle E_{\rm P}\rangle, \end{aligned}$$

where $\langle E_{\rm P}\rangle \equiv \langle \frac{k}{n}(x_i - x_{i-1})^n\rangle$ is the average per-link potential energy. The Boltzmann constant $k_{\rm B}$ has been set to unity. Therefore,

$$\langle E_{\rm P}\rangle = \frac{T}{n}. \tag{7}$$

Since the space translation symmetry has been applied, the above derivation is valid only for homogeneous systems. It looks quite surprising and deserves further study why the conclusion is still exact for such a single interface. In the $n \to \infty$ limit, the result approaches the point $\alpha = \beta = 0$, which is surrounded by the dashed circle in the Fig. 5(a).

To explain $\alpha = 2/n$ is not that straightforward. In the derivation in Ref. [15], it is assumed that the potential energy at the interface $\langle H_{\rm int}\rangle \propto k_{\rm int}$, thus the instantaneous heat current follows $j = fv \propto \frac{\partial H_{\rm int}}{\partial x} \propto k_{\rm int}$, where f and v are the instantaneous force and velocity. Therefore, $\langle j(0)j(t)\rangle \propto k_{\rm int}^2$, which leads to $\langle J\rangle^{\rm st} \propto k_{\rm int}^2$ according to the Green-Kubo formula. Here, we follow the expression in Ref. [15] that $\langle\rangle^{\rm st}$

denotes for the nonequilibrium steady state average (with temperature drop), while the $\langle\rangle$ refers to the equilibrium average. The above derivation is correct for the class one since, as we have shown, $\langle H_{\rm int}\rangle$ indeed decays with $k_{\rm int}$ linearly.

For the class two, however, $\langle H_{\rm int}\rangle$ does not decay with $k_{\rm int}$, but approaches a constant instead. In such a case, $\Delta^2_{\rm int} \propto k_{\rm int}^{-\frac{2}{n}}$, i.e., it follows a power-law divergence in the small $k_{\rm int}$ limit. As $k_{\rm int}$ decreases, the increase of $\Delta^2_{\rm int}$ slows down the decay of the instantaneous heat current j. Quantitatively speaking, $j \propto \frac{\partial H_{\rm int}}{\partial x} \propto k_{\rm int}^{\frac{1}{n}}$. Therefore, when all other factors keep unchanged,

$$\langle j\rangle^{\rm st} \propto \int_0^\infty dt\langle j(0)j(t)\rangle \propto k_{\rm int}^{\frac{2}{n}}. \tag{8}$$

This explains our finding for class two.

V. SUMMARY AND DISCUSSIONS

To summarize, we have systematically studied heat conduction in a few nonlinear lattices, each of which consists of two identical segments that coupled by a weak interface. We focus on the interface strength $k_{\rm int}$ dependence of the heat current J that is induced by a fixed small temperature drop. Existing studies have indicated that in a large amount of systems, J should generally decays by $k^2_{\rm int}$. Our numerical simulations confirmed such a $k^2_{\rm int}$ law in the cases that the mean square relative displacement between the interface particles $\Delta^2_{\rm int}$ approaches either infinity or a finite constat in the small $k_{\rm int}$ limit.

Besides, another class has also been revealed. In this class, J also follows a power-law decay, i.e., $J \sim k^\alpha_{\rm int}$. The power exponent α is, however, not necessarily 2. It is observed that in this class $\Delta^2_{\rm int}$ follows a power-law dependence in the small $k_{\rm int}$ limit too, i.e., $\Delta^2_{\rm int} \sim k^{-\beta}_{\rm int}$. By assuming that the potential energy $E_{\rm P}$ of the interface interaction approaches a non-zero constant, the value of β can be analytically calculated. Based on it, the $k_{\rm int}$ dependence of J in this class can also be analytically explained.

Although the systems that are studied here are all one dimensional, we believe the conclusions can be extended to high-dimensional systems. However, the real interfaces between real materials are possibly even much more complicated, e.g., the Kapitza resistance at the interface between solid and liquid. Therefore, there may also exist different decay classes other than the two that have been revealed.

ACKNOWLEDGMENTS

This work is supported by the National Natural Science Foundation of China under Grant No. 11675262, the Fundamental Research Funds for the Central Universities, and the Research Funds of Renmin University of China 15XNLQ03. Computational resources were provided by the Physical Laboratory of High Performance Computing at Renmin University of China.

[1] E. T. Swartz and R. O. Pohl, Thermal boundary resistance, Rev. Mod. Phys. **61**, 605 (1989).
[2] P. L. Kapitza, The study of heat transfer in helium ii, J. Phys. (USSR) **4**, 181 (1941).
[3] Gerald L. Pollack, Kapitza resistance, Rev. Mod. Phys. **41**, 48 (1969).
[4] I. M. Khalatnikov, Zh. Eksp. Teor. Fiz. **22**, 687 (1952); R. M. Mazo, Theoretical studies on low temperature phenomena, Ph.D. thesis, Yale University, 1955.
[5] P. L. Kapitza, Thermal resistance at interfaces, Appl. Phys. Lett. **51**, 200 (1987).
[6] M. Terraneo, M. Peyrard, and G. Casati, Controlling the Energy Flow in Nonlinear Lattices: A Model for a Thermal Rectifier, Phys. Rev. Lett. **88**, 094302 (2002).
[7] Baowen Li, Lei Wang, and Giulio Casati, Thermal Diode: Rectification of Heat Flux, Phys. Rev. Lett. **93**, 184301 (2004).
[8] Baowen Li, Jinghua Lan, and Lei Wang, Interface Thermal Resistance between Dissimilar Anharmonic Lattices, Phys. Rev. Lett. **95**, 104302 (2005).
[9] Baowen Li, Lei Wang, and Giulio Casati, Negative differential resistance and thermal transistor, Appl. Phys. Lett. **88**, 143501 (2006).
[10] Lei Wang and Baowen Li, Thermal Logic Gates: Computation with Phonons, Phys. Rev. Lett. **99**, 177208 (2007).
[11] Lei Wang and Baowen Li, Thermal Memory: A Storage of Phononic Information, Phys. Rev. Lett. **101**, 267203 (2008).
[12] Nianbei Li, Jie Ren, Lei Wang, Gang Zhang, Peter Hänggi, and Baowen Li, Colloquium: Phononics: Manipulating heat flow with electronic analogs and beyond, Rev. Mod. Phys. **84**, 1045 (2012).
[13] C. W. Chang, D. Okawa, H. Garcia, A. Majumdar, and A. Zettl, Nanotube Phonon Waveguide, Phys. Rev. Lett. **99**, 045901 (2007).
[14] C. W. Chang, D. Okawa, A. Majumdar, and A Zettl, Solid-state thermal rectifier, Science **314**, 1121 (2006).
[15] Dye SK Sato, Pressure-induced Recovery of Fourier's law in one-dimensional momentum-conserving systems, Phys. Rev. E **94**, 012115 (2016).
[16] Ding Chen, S. Aubry, and G. P. Tsironis, Breather Mobility in Discrete φ^4 Nonlinear Lattices, Phys. Rev. Lett. **77**, 4776 (1996).
[17] The value 2.5 guarantees a normal heat conduction with a not-too-small heat conductivity κ in the temperature we shall study [24].
[18] E. Fermi, J. Pasta, and S. Ulam, in *Collected Papers,* edited by E. Fermi (University of Chicago Press, Chicago, 1965), Vol. 2, p. 78.
[19] Stefano Lepri, Roberto Livi, and Antonio Politi, Thermal conduction in classical low-dimensional lattices, Phys. Rep. **377**, 1 (2003).
[20] A. Dhar, Heat transport in low-dimensional systems, Adv. Phys. **57**, 457 (2008).

[21] M. L. James, G. M. Smith, and J. C. Wolford, *Applied Numerical Methods for Digital Computation* (Harper Collins College Publishers, New York, 1993).

[22] Here, the hard means the potential energy diverges in the $x \to \infty$ limit. In contrast, the soft means it is bounded.

[23] Nianbei Li (private communication).

[24] O. V. Gendelman and A. V. Savin, Normal Heat Conductivity of the One-Dimensional Lattice with Periodic Potential of Nearest-Neighbor Interaction, Phys. Rev. Lett. **84**, 2381 (2000).